electronics

MDPI

Article

Phased Array Radar Resource Consumption Method Based on Phase-Switched Screen

Guoqing Hao, Dejun Feng *, Junjie Wang, Zimeng Zhou and Ling Wang

The State Key Laboratory of Complex Electromagnetic Environment Effects on Electronics and Information System, National University of Defense Technology, Changsha 410073, China; haoguoqing21@nudt.edu.cn (G.H.)
* Correspondence: fdj117@nudt.edu.cn; Tel.: +86-13974863862

Abstract: The consumption of phased array radar (PAR) resources affects the accuracy of its multi-target searching and tracking abilities. The jamming methods aimed at PAR involve deceptive jamming and comprehensive jamming strategies, but have the disadvantages of high cost and complexity. Given this context, this paper proposes a PAR resource consumption method based on phase-switched screen (PSS), and derives a relationship between the targets and the evaluation indicators. By implementing periodic modulation of PSS, a controlled number of deceptive multiple false targets can be generated, thereby enticing the radar system to engage in activities such as searching and tracking targets. When the quantity of false targets is increased, the number of beam requests becomes five times higher than compared to the scenario without false targets. This has also led the margin of time resources to exceed 50%, successfully achieving the objective of consuming radar resources. Furthermore, this method offers straightforward manipulation, flexibility, and the potential to significantly consume radar resources. The efficacy of the proposed method is confirmed with the simulation outcomes.

Keywords: phased array radar (PAR); phase-switched screen (PSS); resource consumption; multiple false targets

Citation: Hao, G.; Feng, D.; Wang, J.; Zhou, Z.; Wang, L. Phased Array Radar Resource Consumption Method Based on Phase-Switched Screen. *Electronics* **2023**, *12*, 3750. https://doi.org/10.3390/electronics12183750

Academic Editors: Wensheng Zhao and Jun Wu

Received: 20 August 2023
Revised: 2 September 2023
Accepted: 4 September 2023
Published: 5 September 2023

1. Introduction

Phased array radar (PAR) exhibits the characteristics of multi-beam rapid scanning and shape versatility, facilitating the accomplishment of tasks such as searching, identifying, tracking, and intercepting multiple targets. Its resource management is a major factor affecting its operational performance [1–4].

Consuming radar resources and increasing the workload on the radar will diminish its detection capabilities. An effective way to consume radar resources is to use deception jamming and comprehensive jamming strategies [5–7]. In the jamming of active multiple false targets, Zhou et al. have identified that a vast number of false points or tracks leads to saturation of the PAR system [8]. Zhi et al. have concluded that as the number of false targets increases, the probability of radar detection systems mistaking false targets for real ones also increases [9]. Nevertheless, the methods mentioned above are achieved through active jamming, which still has the disadvantages of high cost and limited flexibility in implementation.

Passive jamming uses angular reflectors and other devices to change the scattering mode of electromagnetic waves, demonstrating the qualities of cost-effectiveness and rapid response [10,11]. However, traditional passive devices possess a singular and fixed electromagnetic property after undergoing processing. In real-time situations, they lack the flexibility to make the necessary adjustments to meet the requirements.

Metamaterials with tunable properties allow for multidimensional and varying degrees of control over the reception of electromagnetic waves by radar systems [12–17]. By

modulating these materials, it becomes possible to alter the radar echo, and thereby influence the accurate measurement of a target's true state. Consequently, they find extensive applications in the realms of stealth and jamming [18–21]. Zhang et al. have introduced three innovative parallel factor techniques that enhance the accuracy of direction of arrival (DOA) estimation [22]. By analyzing the matched filtering characteristics of a phase-switched screen (PSS), Xu et al. have proposed a high-resolution range profile (HRRP) method. This method can not only conceal the real-target's HRRP, but also generate multiple false targets with HRRP characteristics that are highly similar to those of the real target [23]. Wang et al. have utilized PSS to perform intra-pulse and inter-pulse two-dimensional joint non-periodic modulation on the radar reflection signals. This approach allows for the formation of distinct jamming regions in both the range and azimuth dimensions, resulting in a flexible control over the suppression features in the two-dimensional domain after synthetic aperture radar (SAR) image processing [24]. The aforementioned research demonstrates the capability of PSS to generate multiple false targets, thus showcasing promising prospects for its application in the field of radar jamming.

Inspired by the above-mentioned findings, this paper proposes a method for consuming PAR resources through multiple false targets based on PSS. This method utilizes PSS to modulate the incident waves of the radar, generating controlled harmonic components with adjustable spatial distribution and amplitude. These components are considered as multiple false targets generated via electromagnetic modulation, inducing the radar to perform operations such as search and confirmation of targets. The emergence of a large number of false targets leads to an increase in the total number of radar beam requests, resulting in the accuracy and efficiency of target detection and tracking. This significantly affects the normal operation of the PAR, consuming and wasting a portion of the radar resources. Furthermore, this approach offers a greater level of ease in execution and affordability compared to active jamming, and is more flexible and remarkably effective than traditional passive jamming.

The rest of this paper is organized as follows. In Section 2, the theory of PSS electromagnetic regulation is presented. In Section 3, the principle of electromagnetic modulation to generate false targets is proposed. Four basic task types for radar resource scheduling and their evaluation indicators are demonstrated in Section 4. The simulation results and analysis with the resource consumption method are presented in Section 5. Finally, the conclusions are highlighted in Section 6.

2. Electromagnetic Theory of PSS

The PSS structure consists of a switched resistive layer, a dielectric spacer and a conducting back-plane. The switched resistive layer is typically composed of periodically arranged unit structures, with variable impedance components such as positive-intrinsic-negative (PIN) diodes connecting the unit structures, as depicted in Figure 1. The thickness from the surface of the switched resistive layer to the conducting back-plane is denoted as h.

When the bias power supply is loaded onto the switched resistive layer, the variation in the PIN diode resistance within a fixed range can be controlled by manipulating the voltage. When the PIN diode resistance is significantly high, the circuit becomes disconnected, allowing the switched resistive layer to fully transmit the electromagnetic waves. Conversely, when the resistance of the PIN diode becomes exceedingly low, the circuit becomes conductive, resulting in the switched resistive layer exhibiting a full reflection state to the electromagnetic waves.

The control mechanism described above allows for the adjustment of the switched resistive layer's characteristics to effectively control and manipulate the electromagnetic waves as desired. Figure 2 shows the working principle of the PSS. Assume that an electromagnetic wave with a frequency of f_c and a wavelength of λ is incident vertically. The PSS dielectric spacer has a dielectric constant of one. The reflected waves in the completely reflective and completely transmissive states can be denoted as $\cos(2\pi f_c t)$ and $\cos(2\pi f_c t + 2\beta h)$,

respectively, where wavenumber $\beta = 2\pi/\lambda$. When the thickness $h = \lambda/4$, the electromagnetic wave in full transmission state reaches the conducting back-plane and is reflected, then the reflected wave becomes $\cos(2\pi f_c t + 2\beta h) = -\cos(2\pi f_c t)$ [15]. At this point, the phase difference between the reflected wave phase and the incident wave phase is π.

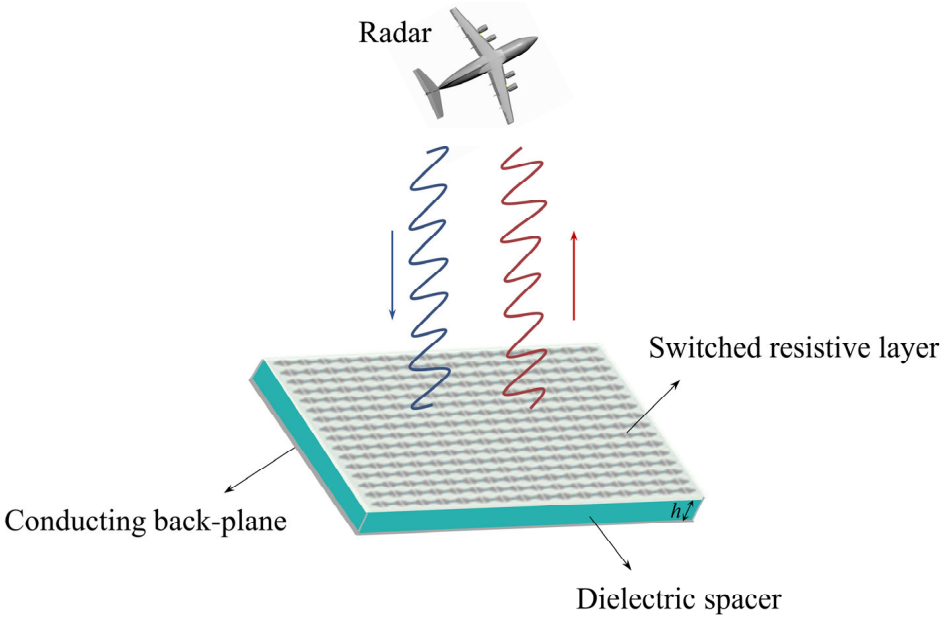

Figure 1. Basic structure of PSS.

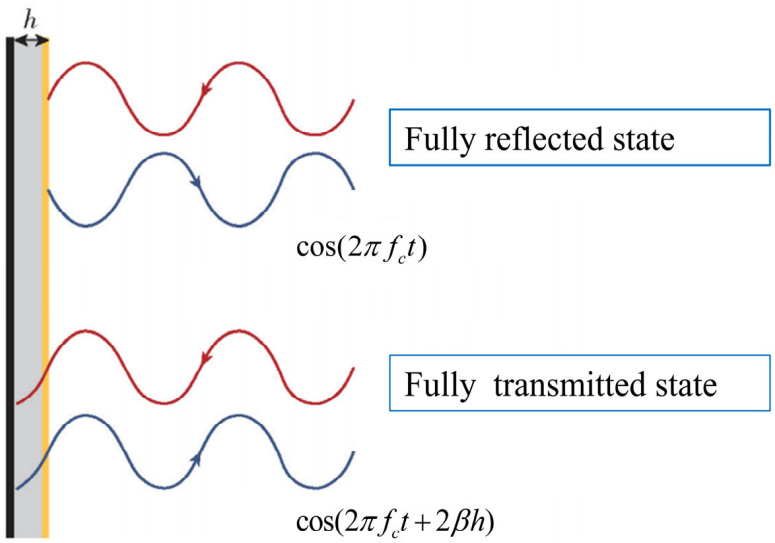

Figure 2. Operating principle of PSS.

Accordingly, periodic switching of the reflection state of the PSS can be realized by controlling the periodic change in the voltage. It is equivalent to multiplying the incident signal by a sequence of bipolar rectangular pulses. The model of the modulated signal for PSS can be observed in Figure 3. The amplitudes correspond to the states of full reflection and full transmission for the PSS, with values of +1 and −1, respectively.

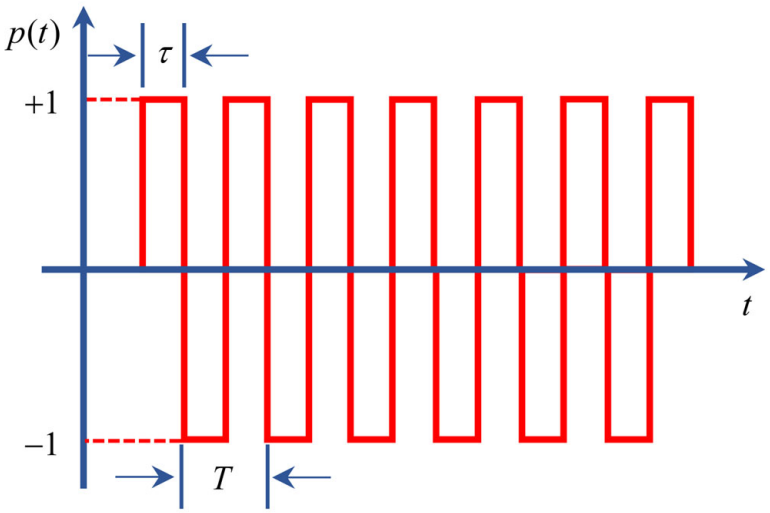

Figure 3. PSS modulation signal model.

The time and frequency-domain PSS modulating signal $p(t)$ and $P(f)$ can be respectively expressed as follows.

$$p(t) = A_0 + \sum_{n=1}^{+\infty} 2A_n \sin(2\pi n f_s t) \tag{1}$$

$$P(f) = \sum_{\substack{n=-\infty \\ n \neq 0}}^{n=+\infty} \left[\frac{\sin(n\pi/2)}{n\pi/2}\right] \delta(f - nf_s) \tag{2}$$

where $A_0 = |2\tau/T - 1|$; $A_n = (1/n\pi)(1 - \cos(2n\pi\tau/T))$; f_s represents the modulating frequency of PSS; and τ/T is the duty ratio of the modulating signal.

When the incident electromagnetic wave $s(t)$ is vertically irradiated onto the PSS, the time domain of its reflected signal can be represented as follows:

$$r(t) = s(t) \times p(t) \tag{3}$$

The representation of the echo signal in the spectral domain is as follows:

$$R(f) = S(f) \otimes P(f) = \sum_{\substack{n=-\infty \\ n \neq 0}}^{n=+\infty} \left[\frac{\sin(n\pi/2)}{n\pi/2}\right] S(f - nf_s) \tag{4}$$

where $\otimes$ represents the convolution of two signals in the frequency domain.

Based on Equation (4), the echo signal modulated by PSS generates multiple harmonic components that are symmetrically distributed around the central frequency. The echoes received by the radar receiver can be regarded as multiple reflected signals with different Doppler frequency shifts, creating numerous false targets.

3. Principle of False Target Generation

The linear frequency modulation (LFM) signal is widely used in radar fields [24]. Assume that the radar transmit signal LFM is denoted as follows:

$$s(t) = \text{rect}\left(\frac{t}{T_p}\right) \exp\left[j2\pi\left(f_0 t + \frac{1}{2}K_r t\right)\right] \tag{5}$$

where T_p represents the signal pulse width, f_0 represents the signal carrier frequency, and K_r represents the signal modulation frequency. $rect(\cdot)$ indicates a rectangular pulse.

Upon the reception of the emitted LFM signal by the radar receiver, it undergoes frequency mixing and correlation filtering processing. The resulting echo baseband signal can be represented as follows:

$$r(t) = rect\left(\frac{t}{T_p}\right)\exp(j\pi K_r t^2) \times \left[A_0 + \sum_{\substack{n=-N \\ n\neq 0}}^{+N} A_n \exp(j2\pi n f_s t)\right] \tag{6}$$

where $N = \lfloor B/f_s \rfloor$; $\lfloor \cdot \rfloor$ means rounded by 0. The baseband signal can be perceived as the amalgamation of numerous LFM signals with alterations induced by the Doppler shift. The ultimate outcome of the matched filtering can be denoted as follows:

$$I_{r(t)} = A_0\left(1 - \left|\frac{t}{T_p}\right|\right)\sin c\left[K_r T_p\left(1 - \left|\frac{t}{T_p}\right|\right)\right] + \sum_{n=-N, n\neq 0}^{+N} A_n\left(1 - \left|\frac{t}{T_p}\right|\right)\sin c\left[K_r T_p\left(t + \frac{nf_s}{K_r}\right)\left(1 - \left|\frac{t}{T_p}\right|\right)\right] \tag{7}$$

In Equation (7), the output that undergoes matched filtering presents numerous sinc discrete peaks, with n denoting the order of said peaks. The output position of the n-th order false target is

$$R_n = \frac{cnf_s}{K_{\mathrm{r}}} \tag{8}$$

where c is the speed of electromagnetic wave propagation in space.

We assume that the length of the reception window in the radar system is d; the number of false targets within range of the receiver is $2n$ when the following equation is satisfied.

$$\frac{2cnf_s}{K_{\mathrm{r}}} \leq d < \frac{2c(n+1)f_s}{K_{\mathrm{r}}} \tag{9}$$

As shown in Equation (9), the number of false targets entering the receiver can be ascertained through the modulation frequency.

The echo signals are subjected to Constant False Alarm Rate (CFAR) detection for target detection after undergoing matched filtering. The widely employed CFAR algorithm is commonly referred to as the Cell Average (CA) CFAR, with its performance in detection typically quantified by detection probability. However, due to the fixed modulation frequency and duty ratio, the false targets generated by PSS exhibit a spatial distribution and magnitude that are relatively stable and do not conform to a random variable. As a result, it is impossible to acquire the probability density function. Therefore, this paper directly utilizes detection thresholds in order to evaluate the detection performance of CFAR.

Assuming that the reference units in CA-CFAR detection amount to $2k_t$, the number of protection units reaches $2k$. In addition, the threshold factor is set as η, allowing for the representation of the detection threshold T_h as follows:

$$T_h(n) = \eta \times \frac{\sum_{i=n-k-kt}^{i=n-k-1} F_s(i) + \sum_{i=n+k+1}^{i=n+k+k_t} F_s(i)}{2k_t} \tag{10}$$

The moment n_1 has

$$T_h(n_1) \leq I_{r(n_1)} \times \sum_{n=t_1}^{n=t_2} \delta(n_1 - nT_s) \tag{11}$$

where $\delta(t)$ represents an impulse function, and the right-hand side of this equation is the sampling function of the matched filter at moment n_1. This implies that the false targets have passed radar detection.

The presence of false targets detected by the radar tempts it to engage in tracking and confirmation operations, thus leading to a waste of radar resources.

4. Radar Resource Scheduling and Its Evaluation Indicators

The vigorous development of PAR technology has fully demonstrated its ability to detect and track various types of targets flexibly, rapidly and multifunctionally. PAR can form hundreds of tracking and searching beams in a short time, and carry out echo processing. This enables the radar to operate simultaneously on multiple targets conducting searching, tracking, confirming, anti-jamming and other modes of operation.

Each radar task will consume radar resources, but radar resources are limited. Therefore, the eallocation and use of these resources will be of great significance in realizing the great potential of phased array radar.

Radar event scheduling determines beam pointing and the type of event to be executed at each moment, according to certain principles. Within each scheduling event, the time and energy resources occupied by each task are also different. Generally, four radar mission types are included in phased array radars [2,4]:

1. Search task request: It is also known as routine search or conventional search. This task completes beam scanning coverage of the surveillance airspace in a preset scanning pattern for a given period of time.
2. Track task request: This is a tracking irradiation and track correlation process for a confirmed track at a given data rate.
3. Confirm task request: Based on the results of the search task, the task confirms the detection of the generated new start tracks to confirm whether the target is false or not. It is also necessary to establish the search-to-track process to complete the closure of the tracking loop in the distance and angle dimensions.
4. Lost-process task request: The task conducts supplementary searches for lost targets. It is usually centered on the beam request position and follows a number of wave positions.

In this paper, the number of radar beam requests and the time resource margin of a PAR system are used as indicators to assess the resource consumption of phased array radars.

4.1. Number of Radar Beam Requests

In each resource scheduling process, the radar schedules the list of beam requests in order of priority. The prioritization of the four tasks is shown in Table 1. When there are a large number of requests for the other three types of beams, it is possible to have a situation where the search task can never be scheduled. To ensure that the search of the surveillance airspace is performed in each scheduling, a routine search task for each scheduling cycle is set up.

Table 1. Prioritization of radar task requests.

Type of Request	Level of Priority
Track task request	1
Confirm task request	2
Lost-process task request	3
Search task request	4

The number of radar beam requests represents the total count of irradiation requests made to the radar scheduling system, which encompasses four types of radar request events. It represents the burden on the radar resource scheduling system. An increase in the number of beam requests places higher demands on the radar data processing system.

In this paper, the calculation of this indicator does not include the number of search requests since search events are considered routine tasks that occur in each period. Additionally, lost-process events are not considered due to their infrequent occurrence in the simulation.

Assume that the radar detects K_i targets at the i-th scheduling. The radar track processing process uses the 'm/n' rule of the logic method and the average probability of successful confirmation is $\overline{P_c}$. The number of confirmation request events N_{CQ} caused by this irradiation is

$$N_{CQ} = K_i(n - \overline{P_c}n + \overline{P_c}m) \tag{12}$$

The number of tracking request events N_{TQ} in this radar dwell time period $\overline{\Delta t}$ is

$$N_{TQ} = \overline{P_c}\lfloor N_{Ci}/n \rfloor \overline{\Delta t} \tag{13}$$

where N_{Ci} denotes the number of confirmation irradiations in a total of i-th scheduling.

After I-th scheduling, the total number of radar beam requests is at least

$$N_Q = \sum_{i=1}^{I}\left(N_{CQ} + N_{TQ}\right) = \sum_{i=1}^{I}\left(K_i(n - \overline{P_c}n + \overline{P_c}m) + \overline{P_c}\lfloor N_{Ci}/n \rfloor \overline{\Delta t}\right) \tag{14}$$

4.2. Time Resource Margin for Phased Array Radar Systems

The system resources of the PAR are prioritized to accomplish the higher priority radar tasks. In the simulation system, the search task is considered a resident task and therefore has the lowest priority [4]. The ratio between the time consumed by the search task and the overall system time resources can indicate the current saturation level of the system. It is defined as the time resource margin R_t of the PAR system, which is expressed as

$$R_t = 1 - \frac{T_s}{T_a} \tag{15}$$

where T_s denotes the time consumed by the search task; T_a denotes the system time resource.

In this paper the beam dwell time for all four tasks is $\overline{\Delta t}$, so the number of tasks can be used instead of the task time. So the above equation can be changed to

$$R_t = 1 - \frac{n_s\overline{\Delta t}}{(n_s + n_c + n_t + n_l)\overline{\Delta t}} = 1 - \frac{n_s}{n_s + n_c + n_t + n_l} \tag{16}$$

5. Simulation Analysis

5.1. Simulation Parameter Setting

This section employs a simulation analysis to substantiate the aforementioned proposed approach of utilizing electromagnetic modulation materials for radar resource consumption. The simulation parameters are presented in Table 2. The quantity of real targets in the simulated environment totals eight, and they consistently sustain a uniform linear motion.

Table 2. Simulation parameters.

Parameter	Value (Unit)	Parameter	Value (Unit)
Number of search requests	23	Signal bandwidth (B)	10 (MHz)
Carrier frequency (f_0)	6 (GHz)	Protection units	8
Pulse duration (T_p)	50 (us)	Reference units	64
Chirp rate (K_r)	2×10^{11} (Hz/s)	Logical method	2/3

5.2. Generation of False Targets

In accordance with the fundamental principle of target electromagnetic modulation outlined in Section 2, the PSS changes the radar echo by actively modulating the electromagnetic wave. Based on this, it can generate false targets and consume radar resources. From the principle analysis, the key parameters of PSS-modulation include duty ratio and modulation frequency. They affect the relative magnitude and the spatial distribution between the individual false targets, respectively. This short section will verify this principle through simulation. The simulation is performed using MATLAB software, and the target movement time is 20 s. Figure 4 shows the curves of envelope detection and CFAR detection threshold under different modulation parameters.

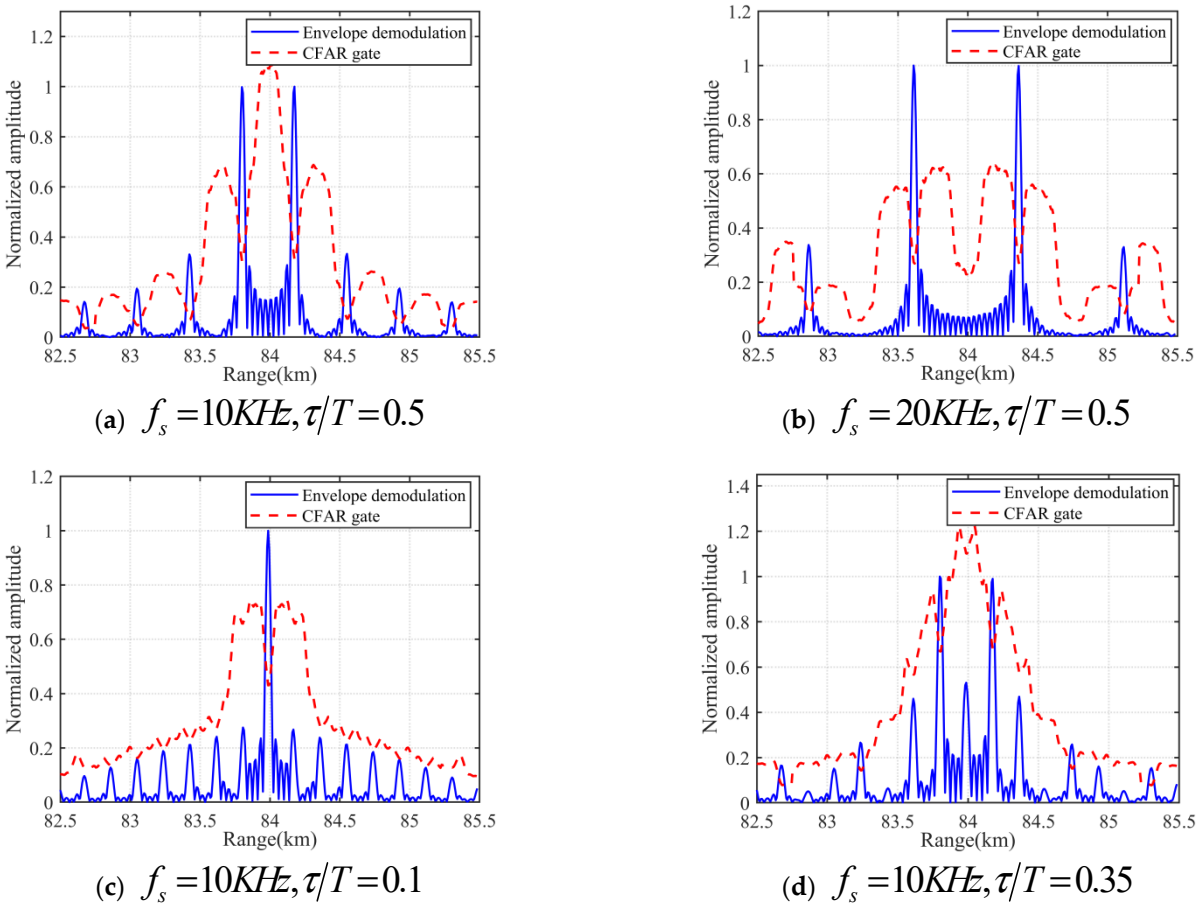

Figure 4. The quantity of false targets passed while adjusting different modulation parameters.

The blue curve in the figure shows the output of the target envelope demodulation, where the peaks represent different targets. Only the one in the center is the real target; the rest are false targets generated with the PSS modulation.

From Figure 4a–d, it can be seen that under the modulation effect of PSS, multiple peaks appear in the modulated radar envelope demodulation. These peaks are symmetrically distributed from the real target.

When the duty ratio is 0.5, as shown in Figure 4a,b, the output has almost no energy at the center, which means that the real target has faded. The spatial arrangement of false targets is influenced by the modulation frequency. An increase in the modulation frequency leads to an increase in the separation among the false targets.

Based on Figure 4a,c,d, it can be concluded that the change in duty cycle changes the amplitude of the false targets of each ordere. However, the spatial distribution of the multiple false targets generated by the PSS modulation in the three cases does not change. Comparison of the three figures shows that the fluctuation of detection thresholds is caused

by variations in the amplitudes of false targets. A moderate increase in the duty ratio within the range of 0–0.5 allows more false targets to surpass detection, enhancing the effectiveness of modulation. In Figure 4d, the envelope demodulation has some energy at the center. The false targets on either side of it have a higher amplitude, which causes the real target to fail radar detection.

In summary, the duty ratio and modulation frequency have an impact on the amplitude and spatial distribution of multiple false targets, respectively, which in turn affects the quantity of false targets detected through the radar. This determines the effect of consuming radar resources, so the following section entails an examination of the impact of modulation parameters on radar resource consumption via simulation.

5.3. Impact of Duty Cycle on the Number of Beam Requests

To further analyze the impact of the modulation duty ratio on resource consumption, the simulation keeps the modulation frequency constant while varying the modulation duty ratio of the PSS modulation signal. In Figure 5, the relationship curve between the number of beam requests and false targets is depicted as the modulation duty ratio changes with a constant modulation frequency of 10 KHz.

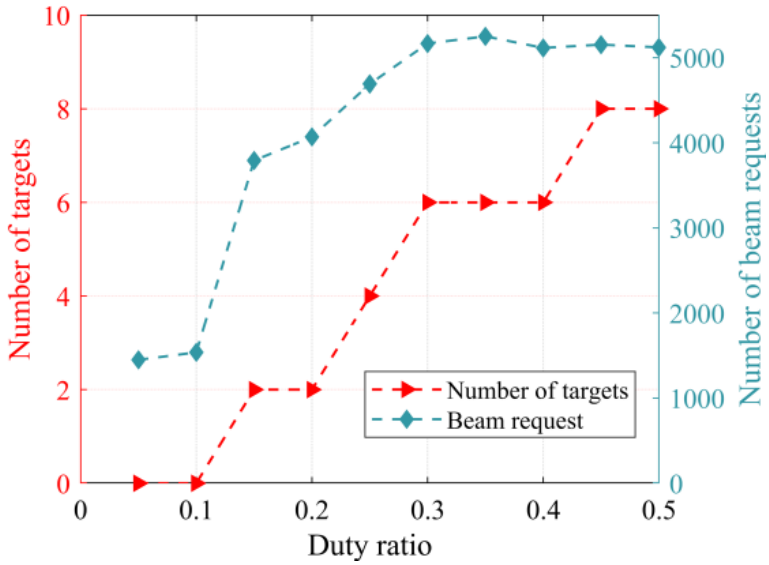

Figure 5. The impact of duty ratio on the number of beam requests and false targets.

Based on the principle of PSS modulation, it is known that the modulation effect of PSS is symmetrically distributed around 0.5. So only the simulation results of 0–0.5 are given in this paper.

As depicted in Figure 5, all false targets generated in the 0.05–0.1 range failed to pass radar detection. Both the number of false targets and beam requests in the range 0–0.5 increase with increasing duty ratio. This indicates an increase in the number of beam requests multiplied when faced with the occurrence of multiple false target jamming, resulting in a significant increase in the radar's workload. At a duty ratio of 0.3–0.5, the number of beam requests remains relatively stable. This limitation arises from the simulation's predefined maximum number of tasks that can be executed within each scheduling period, resulting in a limitation of the total number of beam requests. Therefore, the presence of excessive false targets can jam the radar's normal operation on real targets, particularly when system resources are limited.

5.4. Impact of Modulation Frequency on the Number of Beam Requests

This analysis delves into the impact of modulation frequency variations on resource consumption. Figure 6 shows the correlation curve between the modulation frequency and the quantity of false targets and the number of beam requests when the modulation duty ratio is 0.5.

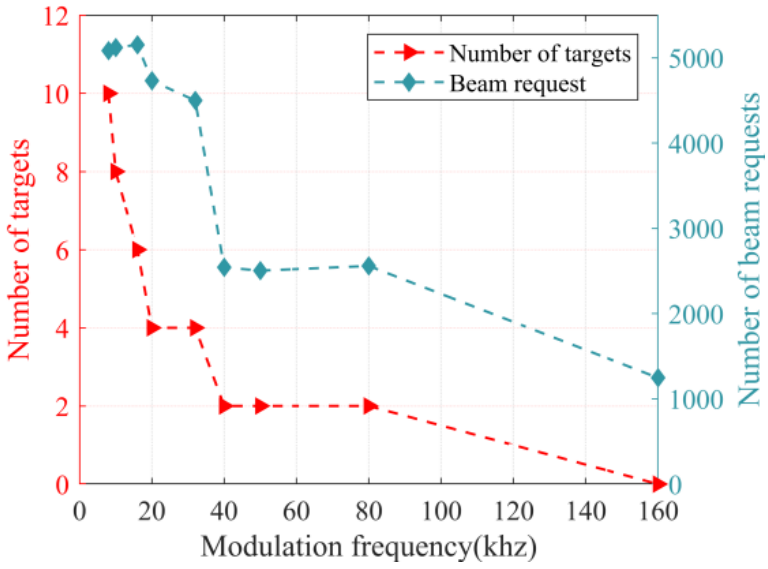

Figure 6. The impact of modulation frequency on the number of beam requests and false targets.

As shown in Figure 6, as the modulation frequency increases, the quantity of false targets and beam requests correspondingly diminishes. The variation in the number of beam requests is more evident at lower modulation frequencies. According to the modulation principle, it can be seen that the modulation frequency affects the spatial distribution of false targets. When the modulation frequency is lower, the false targets are more densely spaced. Lowering the modulation frequency causes more false targets to enter the radar receiver, which in turn generates more beam requests to consume radar resources. When the modulation frequency increases from 40 KHz to 80 KHz, the quantity of false targets entering the radar receiver remains the same. This occurs due to the fact that only the primary false targets fall within the bandwidth of the radar receiver. Hence, the change in the number of beam requests is also insignificant. The number of beam requests peaks when four false targets or more are generated around each real target. At this point, the radar burden is maximized, resulting in a possible failure to confirm or track the emerging targets. This leads to the consumption and waste of radar resources.

Based on the above analysis, it can be concluded that the quantity of false targets detected is affected by fluctuations in modulation frequency and duty ratio. Ultimately, it affects the number of beam requests generated. So to get the desired consumption effect, it is necessary to consider both modulation duty ratio and frequency.

5.5. Impact of the Number of Multiple False Targets on the Margin of Time Resources

The resource margin of radar time is also an important indicator to assess how much radar resources are consumed. In order to further analyze the consumption effect under multiple false targets generated by electromagnetic modulation materials, PSS is simulated to generate different numbers of false targets to consume radar resources. Figure 7 shows the relationship curve of radar time resources under different numbers of false target jamming.

The graph shows that the time resource stabilizes after a certain period of time. It is because the radar has found all the targets, and at this point no new targets appear, including false targets. A large population of false targets would increase the resources

the radar uses for non-search task, while search resources would be forced to decrease. This means that the radar's ability to monitor the airspace is reduced, possibly resulting in delayed detection of emerging targets. As more targets come into the radar search range, other types of radar tasks gradually grab time resources for search events due to the prioritization principle in the scheduling guidelines. The time resources for other tasks exceeded a maximum of fifty percent, severely affecting the radar's search function.

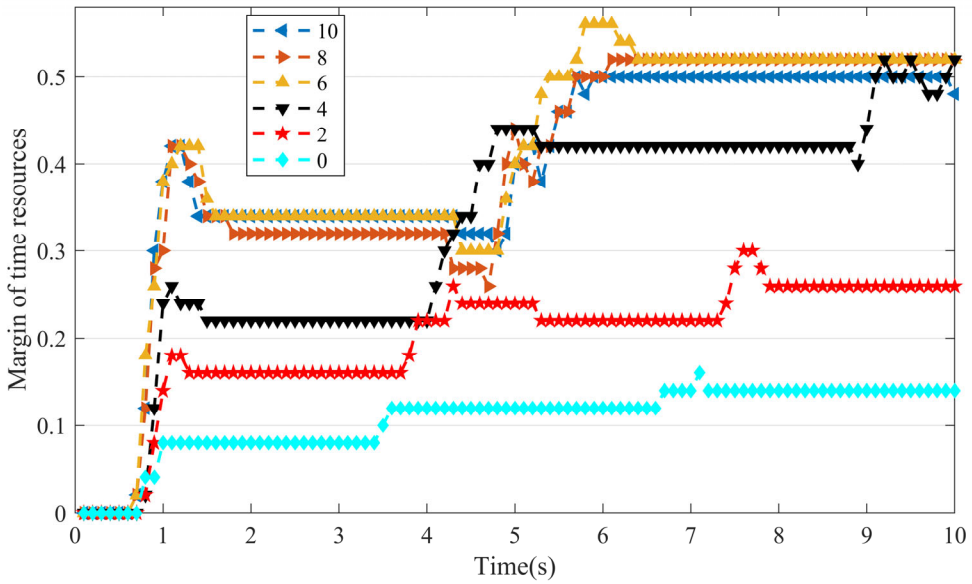

Figure 7. The influence of target number on the margin of time resources.

6. Conclusions and Future Works

This paper presents a method for consuming radar resources by generating multiple false targets based on PSS. Firstly, the electromagnetic modulation principle and false target generation principle of PSS are introduced. Then, the requirements for CFAR detection are analyzed. By adjusting the parameters of the PSS, the quantity of false targets detected by the radar can be controlled. To explore the impact of crucial modulation parameters on the number of beam requests, a series of simulation experiments are conducted. The experimental results are compared by setting distinct modulation frequencies and duty ratios. Furthermore, this paper examines the variations in the margin of time resources under different numbers of false targets. The simulation findings indicate that the quantity of false targets is directly proportional to the number of beam requests. The increase in the number of false targets leads to the beam request count surpassing 5000; the request count even becomes efive times more than the number when there are no false targets. The margin of time resources exceeds 50%, significantly impeding the radar's search capabilities. This method allows for the flexible control of the quantity of multiple false targets by adjusting the controlled materials, thereby controlling the consumption of radar resources. The effectiveness of this method is validated through the simulation of PAR operation process utilizing PSS modulation.

The method presented in this paper possesses the advantage of generating multiple false targets with flexible control. Compared to active jamming and conventional passive jamming, this method is characterized by its agility, efficiency, and a reduction in operational complexity in real-world applications; it is feasible to place the PSS on the surface that is being protected to consume radar resources. Further research should be conducted to carry out additional experimental validations, with the aim to verify the feasibility and practicality of this method in real radar systems and to evaluate its effectiveness.

Author Contributions: Conceptualization, G.H. and L.W.; Data curation, J.W. and L.W.; Formal analysis, G.H. and Z.Z.; Funding acquisition, J.W.; Investigation, Z.Z.; Methodology, D.F.; Project administration, D.F., J.W. and L.W.; Resources, D.F. and J.W.; Software, G.H.; Supervision, D.F. and L.W.; Validation, G.H. and Z.Z.; Visualization, G.H. and Z.Z.; Writing—original draft, G.H.; Writing—review and editing, J.W. All authors have read and agreed to the published version of the manuscript.

Funding: This research was funded by the National Natural Science Foundation of China, grant number 62201589, 62371455.

Data Availability Statement: The data that support the findings of this study are available from the corresponding author upon reasonable request.

Conflicts of Interest: The authors declare no conflict of interest.

References

1. Zhang, G.; Zhao, Y. *Phased Array Radar Technology*; Publishing House of Electronics Industry: Beijing, China, 2006; pp. 32–140.
2. Hu, W.; Yu, W.; Lu, J. *Theories and Methods of Phased Array Radar Resource Management*; National Defense Industry Press: Beijing, China, 2011; pp. 28–50.
3. Lu, J. Theory and Method of Resource Optimization and Management for Phased Array Radars. Ph.D. Thesis, National University of Defense Technology, Changsha, China, 2007.
4. Wang, X.; Xiao, S.; Feng, D. *System Modeling and Simulation of EW of Modern Radar*; Publishing House of Electronics Industry: Beijing, China, 2010; pp. 234–353.
5. Tao, T.; Zhang, G.; Leung, H. An Optimal Algorithm of Time Resource for Multi-Target Tracking under Active Oppressive Jamming. In Proceedings of the 2019 IEEE International Conference on Signal Processing, Communications and Computing (ICSPCC), Dalian, China, 20–22 September 2019.
6. Lang, W.; Mei, S.; Liu, Y.; Zhou, F.; Yang, X. A Periodic Multiple Phases Modulation Active Deception Jamming for Multistatic Radar System. *IEEE Trans Aerosp Electron Syst.* **2023**, *59*, 3435–3451. [CrossRef]
7. Jiang, X.; Zhou, F.; Chen, S.; He, H.; Yang, J. Jamming Resilient Tracking Using POMDP-Based Detection of Hidden Targets. *IEEE Trans. Inf. Forensics Secur.* **2021**, *16*, 983–998. [CrossRef]
8. Zhou, Y.; Shi, L.; Chen, M.; Zhao, F.; Wang, X. Optimized resource management for phased array radar in dense jamming. *Acta Electron. Sinica* **2005**, *33*, 999–1003.
9. Zhi, S. Research on Deception Jamming to Phased Array Radar. Master's Thesis, Xidian University, Xian, China, 2012.
10. Díaz-Rubio, A.; Tretyakov, S. Angular response of anomalous reflectors: Analysis and design prospects. In Proceedings of the 2021 15th European Conference on Antennas and Propagation (EuCAP), Dusseldorf, Germany, 22–26 March 2021.
11. Luo, Y.; Guo, L.; Zuo, Y.; Liu, W. Time-Domain Scattering Characteristics and Jamming Effectiveness in Corner Reflectors. *IEEE Access* **2021**, *9*, 15696–15707. [CrossRef]
12. Guo, Y.; Li, G. Energy-Selective-Surface-Based Dynamic Phase Modulation Surface. *IEEE Antennas Wirel. Propag. Lett.* **2022**, *21*, 1363–1367. [CrossRef]
13. Wang, D.; Yin, L.; Huang, T.; Han, F.; Zhang, Z. Design of a 1 Bit Broadband Space-Time-Coding Digital Metasurface Element. *IEEE Antennas Wirel. Propag. Lett.* **2020**, *19*, 611–615. [CrossRef]
14. Dai, J.; Zhao, J.; Cheng, Q.; Cui, T. Independent Control of Harmonic Amplitudes and Phases via a Time-Domain Digital Coding Metasurface. *Light Sci. Appl.* **2018**, *7*, 888–897. [CrossRef] [PubMed]
15. Zhang, R. Research on the Properties and Radar Effect of Phase Switched Screen. Master's Thesis, National University of Defense Technology, Changsha, China, 2016.
16. Tennant, A.; Chambers, B. Experimental performance of a phaseswitched screen against modulated microwave signals. *IEEE Proc. Radar Sonar Navigat.* **2005**, *152*, 29–33. [CrossRef]
17. Ramaccia, D.; Sounas, D.L.; Alu, A.; Toscano, A.; Bilotti, F. Phase-induced frequency conversion and Doppler effect with time modulated metasurfaces. *IEEE Antennas Wirel. Propag.* **2020**, *68*, 1607–1617. [CrossRef]
18. Phon, R.; Ghosh, S.; Sungjoon, L. Novel multifunctional reconfigurable active frequency selective surface. *IEEE Trans. Antennas Propag.* **2018**, *67*, 1709–1718. [CrossRef]
19. Chang, Y.; Wang, L.; Li, B.; Jiao, W. Phase Switched Screen for Radar Cloaking Based on Reconfigurable Artificial Magnetic Conductor. *IEEE Trans. Electromagn. Compat.* **2021**, *63*, 1417–1422. [CrossRef]
20. Xu, L.; Feng, D.; Wang, X. Matched-filter properties of linear-frequency-modulation radar signal reflected from a phase-switched screen. *IET Radar Sonar Navig.* **2016**, *10*, 318–324. [CrossRef]
21. Xu, H.; Quan, Y.; Zhou, X.; Chen, H.; Cui, T. A Novel Approach for Radar Passive Jamming Based on Multiphase Coding Rapid Modulation. *IEEE Trans. Geosci. Remote Sens.* **2023**, *61*, 1–14. [CrossRef]
22. Zhang, Z.; Wen, F.; Shi, J.; He, J.; Truong, T.K. 2D-DOA Estimation for Coherent Signals via A Polarized Uniform Rectangular Array. *IEEE Signal Process. Lett.* **2023**, *30*, 893–897. [CrossRef]

23. Xu, L.; Feng, D.; Zhang, R.; Wang, X. High-Resolution Range Profile Deception Method Based on Phase-Switched Screen. *IEEE Antennas Wirel.* **2016**, *15*, 1665–1668. [CrossRef]
24. Wang, J.; Feng, D.; Sui, R.; Xing, S.; Xiao, S. Research on Manipulation Method of SAR Target Feature Based on Phase-Switched Screen. *Acta Electron. Sinica.* **2023**, *51*, 564–572.